The Effect of Upper Nozzle Refractory in Bubble Behavior Inside the SEN and Slab Mold in Continuous Casting: Physical and Mathematical Model

Paulo Luiz Santos Junior[1], Johne Jesus Mol Peixoto[2], Carlos Antônio da Silva[2], Itavahn Alves da Silva[2], Clenice Moreira Galinari[3], Varadarajan Seshadri[4]

[1]RHI Magnesita / Department of Metallurgical Engineering - Pontifical Catholic University of Minas Gerais, Praça Louis Ensch, 240, Contagem, MG, Brazil, 32210-902.
Phone: (+55) 31 991985734
Email:paulo.luiz@pucminas.br

[2]Department of Metallurgical Engineering and Materials, Federal University of Ouro Preto, Morro do Cruzeiro, Ouro Preto, MG, Brazil, 35400-000
Phone: (+55) 31 35591101
Email: johnepeix@yahoo.com.br; casilva@ufop.edu.br; itavahnufop@yahoo.com.br;

[3]RHI Magnesita,
Praça Louis Ensch, 240, Contagem, MG, Brazil, 32210-902.
Phone: (+55) 31 988662486
Email: clenice.galinari@rhimagnesita.com

[4]Department of Metallurgical Engineering and Materials, Federal University of Minas Gerais
Av. Antonio Carlos 6627, Belo Horizonte, MG, Brazil, 31.270-901
Phone: (+55) 31 32861854
Email: seshadri@demet.ufmg.br

Abstract

This study intends to investigate the behavior of gas bubbles (air) inside a liquid flow system, simulating the submerged-entry nozzle (SEN) refractory system, using a physical model. Air was injected through porous refractory plates, produced by RHI Magnesita, inside a water channel simulating the SEN. Recording was done with a high-speed camera (1000 frames/second) in order to assess gas distribution. Based on this, a mathematical model has been developed with the objective of evaluating the effect of flow rate (gas-liquid) on gas distribution for different combinations of drag and non-drag forces. The effect of gas distribution on the flow field of liquid inside the mold and other metallurgical aspects were discussed.

Keywords: Physical Modelling; CFD; Continuous Casting; Upper Nozzle; Refractory; Non drag forces.

INTRODUCTION

In the last decades, there has been continuous demand in the automobile industry in respect of particularly ultra low carbon steels and other special steels. In addition to ultra low carbon content in steel, the steel after refining and continuous casting end product should be defect free having a high degree of cleanliness so that during the rolling, stamping and painting processes surface defects and others don't show up leading to inferior product quality and rejections, leading to lower productivity. This aspect of stringent quality of products has led to considerable progress in quality control and innovations in continuous casting, and subsequent production of plates as well as in refractory production and use in the various stages of these high temperature processing technologies.

According to Suzuki [1] and Yuan [2], in the production of steel via continuous casting, the injection of argon (Ar) through the refractories, mainly through the upper nozzle, plays a fundamental role in controlling the obstruction and improving the surface temperature of the steel in the mold as well as promoting separation of non-metallic inclusions. On the other hand, when the air bubbles become trapped in the solidification front during casting, they can lead to internal defects in the

processing of steel. In this context, Suzuki [1] demonstrates that the size of the gas bubbles injected into the upper nozzle and then released by the outlet of the submerged entry nozzle (SEN) into the mold depends on the porous material, the gas injection rate, fluid velocity, SEN geometry and configuration.

Thomas [3], in turn, observed in a physical model of a continuous casting pouring system, with single pore gas injection in the upper nozzle region, that injected gas presented different bubble shapes and behaviors depending on flow rate of water and gas injection rate. For example, for low flow rates of water and low gas injection rates, there was uniform formation of spherical bubbles, smoothly released and accompanying the flow of the liquid. While, for intermediate gas flow rates the same remained close to the wall and the bubbles were normally elongated.

Lee et al. [4]investigated the initial behavior of bubbles in a water model using porous MgO refractory coated samples to simulate the upper nozzle and the steel-argon contact with different permeabilities through filming the upper nozzle region with high-speed camera (4,000 frames per second). The size of the bubble tends to reduce with increasing liquid velocity and tends to become larger with increasing gas injection rate. Another relevant point is that the use of porous materials with varying pore size distributions allows to modify the average size of the bubble. This behavior was also confirmed by Santos et al. [5] in a dynamic and static physical model with the use of refractories with different porosities.

Liu and Thomas [6] pointed out that for the gas to be released from the refractory/liquid interface into the liquid, a pressure rise is required to overcome the surface tension forces in order to increase the curvature. However, for dynamic systems the fluid flow has a decisive effect on the size of the bubble, i.e., for higher flow rates the bubble is released from the surface of the refractory in advance with a smaller bubble diameter than in the case of reduced flow rates or in a static condition.

This study intends to investigate the behavior of inert gas bubbles inside a liquid flow system, simulating the SEN refractory system, using a physical model. Air was injected through porous refractory plates, produced by RHI Magnesita, inside a water channel simulating the SEN. Recording was done with a high speed camera at 1000 frames/second (fps) in order to assess bubble size and distribution and the results were discussed. Based on that a mathematical model was setup to evaluate the effect of flow rate of gas and liquid as well as non-drag forces such as wall lubrication force (WLF), turbulent dispersion force (TDF) and virtual mass force (VMF) on gas distribution. The consequences of gas distribution in the flow field inside the mold and metallurgical aspects were discussed.

Methods and Materials

a) Refractory Production and Characterization

The refractory plates were manufactured by RHI Magnesita Research Center laboratory in the dimensions of 40x160x60mm. They are porous refractories used in industrial applications, according to industrial recipes. Subsequently, in order to reduce variability, the firing of these parts was carried out in tunnel furnaces among other industrial parts. More details about the refractories were presented in a previous publication [5].

As so the refractories used in the experiments were characterized according to the norms and procedures established for industrial products. The main results (average values) are given in Table 1.

Table 1: Physical properties of porous materials used in physical model experiments

Property	Value
Bulk Density BD (g/cm3)	2.87
Apparent Porosity AP (%)	26.43
Cold Crushing Strength CCS (MPa)	78.06
Permeability (CentiDarcy - cD)	928.00

b) **Physical Modelling and Experimental Procedure**

The channel physical model was built using a porous brick similar to those used in an actual casting machine. Care was taken in order to have the same approximate cross section area of the channel as compared with the industrial nozzle. The same holds for liquid (water) flow rate and gas specific flow rate (STP liter per minute per square meter). Thus the operational range includes conditions which are similar to industrial practice. This model was built in order to assess calibration data (to assess the coefficients of Virtual Mass, Lift, Wall Lubrication forces). Similarity does not need to be perfect and it is important to simulate a wide range of conditions. The difference between the inlet and outlet diameter has been purposely established to reproduce the backpressure of the refractory/ mold system in the continuous casting. The central area has been modified to allow a better evaluation and calibration of drag and non-drag forces. A perfect reproduction of the geometry of the SEN did not allow an adequate evaluation of the non-drag forces [5]. The flat refractory plates were mounted in a way to allow the homogeneous injection of gas on opposite sides representing the upper nozzle.

Upwards or downwards flow conditions are assessed in order to better evaluate buoyancy effects. The channel model is depicted in Figure 1.
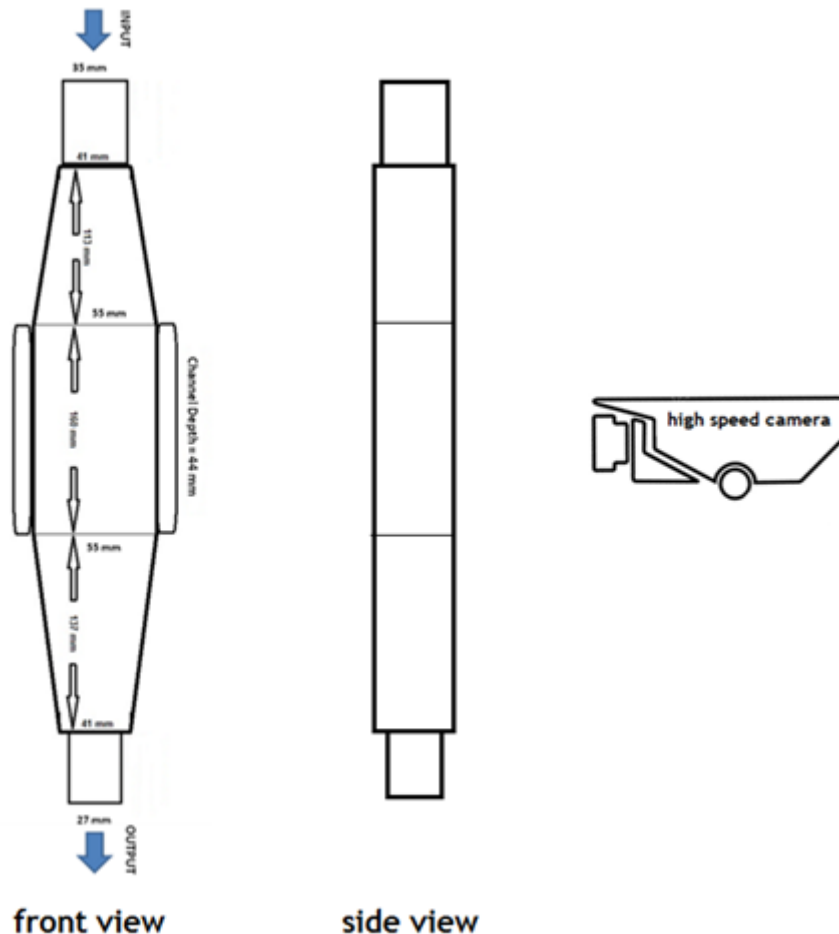

Figure 1: Physical model in acrylic with dimensions and locations of refractory plates in the model (front view) and camera positioning(side view)

The water flow rates used were 40, 60 and 80 l/min. The water flow rate was adjusted with the aid of a Rosemount magnetic flowmeter and frequency inverter for pump rotation control. The air injection rates used were 2 and 5STPl / min. Gas flow control was performed using pressure regulators and OMEGA mass flow meter of the FMA series.

Filming was performed using a high-definition and high velocity AOS S-PRI camera incorporated in the physical model. The video capture was done at 1000fps in order to have an overview of the behavior of water-gas fluid interaction for calibration and subsequent validation of the mathematical model.

c) **Mathematical Modeling**

A first set of CFD simulations was performed in order to reproduce the gas distribution depicted in the physical model. The main objective was to assess parameters for non-drag forces such as wall lubrication force (WLF), turbulent dispersion force (TDF) and virtual mass force (VMF). Due to its symmetrical geometry and the objective of saving computational resources, only half of the model was taken for simulation purposes, see figure 2 – a. The mathematical model for non-drag forces validation and its influence on the distribution of dispersed air (volumetric fraction) in the continuous phase of water was constructed with the same dimensions of the physical model. Water flow rates of 40, 60 and 80lpm with flow rates of 1, 2 and 5STPl / min of air have been taken in consideration. Based on results discussed and presented by Peixoto et al. [7], the parameters evaluated were VMF, TDF and WLF (Liu et al. [8]). For validation the fixed size bubble condition was used to simplify the mathematical calculations and then a comparison between fixed bubble size and MUSIG scheme was done. Liu et al. [8] also described the equations of lift forces, VMF, TDF and WLF and then used a MUSIG function to develop a mathematical model of bubble interaction in a mold of slab in continuous casting.

The second set of simulation comprised a full scale (1:1) water –air system working under Froude number similarity criterion (essentially same flow rate), see Figure 2-b. The mathematical model of continuous casting was elaborated in such a way as to represent the physical conditions of the model in water with respect to the actual dimensions of the model. The water flow used was 336L / min and 400L / min with the air flow rate of 12 STPl / min (Santos et al [9]). The mesh was constructed with 350,400 nodes, being more refined at the outlet of the submerged nozzle and in the jet region (Figure 2 b).

In both cases the software used was the CFX in permanent transient module (CFX 17.1 , Ansys®). The mathematical model considers the three-dimensional and turbulent flow; incompressible Newtonian fluids (the expansion of the gas was not considered), isothermal system (at 25ºC), ambient pressure equal to 1atm. Standard values for the physical properties of water and air (at 25°C) were used. The interfacial tension between gas and water was taken as 0.0728 N/m with consideration of the buoyancy force for the dispersed phase. Water was defined as continuous phase; air, ideal gas, as the dispersed phase.

The mesh was built with a maximum element size of 1 mm. Inflation was used on the walls in order to obtain a better fit for the calculation of the turbulence equations in this region.

For the description of the velocity field, **k-ε** model was used, embedded in ANSYS®. In this model, k represents the kinetic energy of turbulence, defined by the velocity fluctuations and **ε** is the dissipation rate of turbulent kinetic energy. The equations are solved interactively, until convergence, considering the characteristic boundary conditions of the system. The kinetic energy of turbulence and the rate of energy dissipation at the inlet are determined from the average velocity in the system, ie by the flow and cross-sectional area of flow. At the walls non-slip condition has been assumed, which implies kinetic energy of turbulence, kinetic energy dissipation rate of turbulence and velocity are zero. In the output, region of the mixture water and gas, the variables are free to float being therefore determined by the mathematical code.

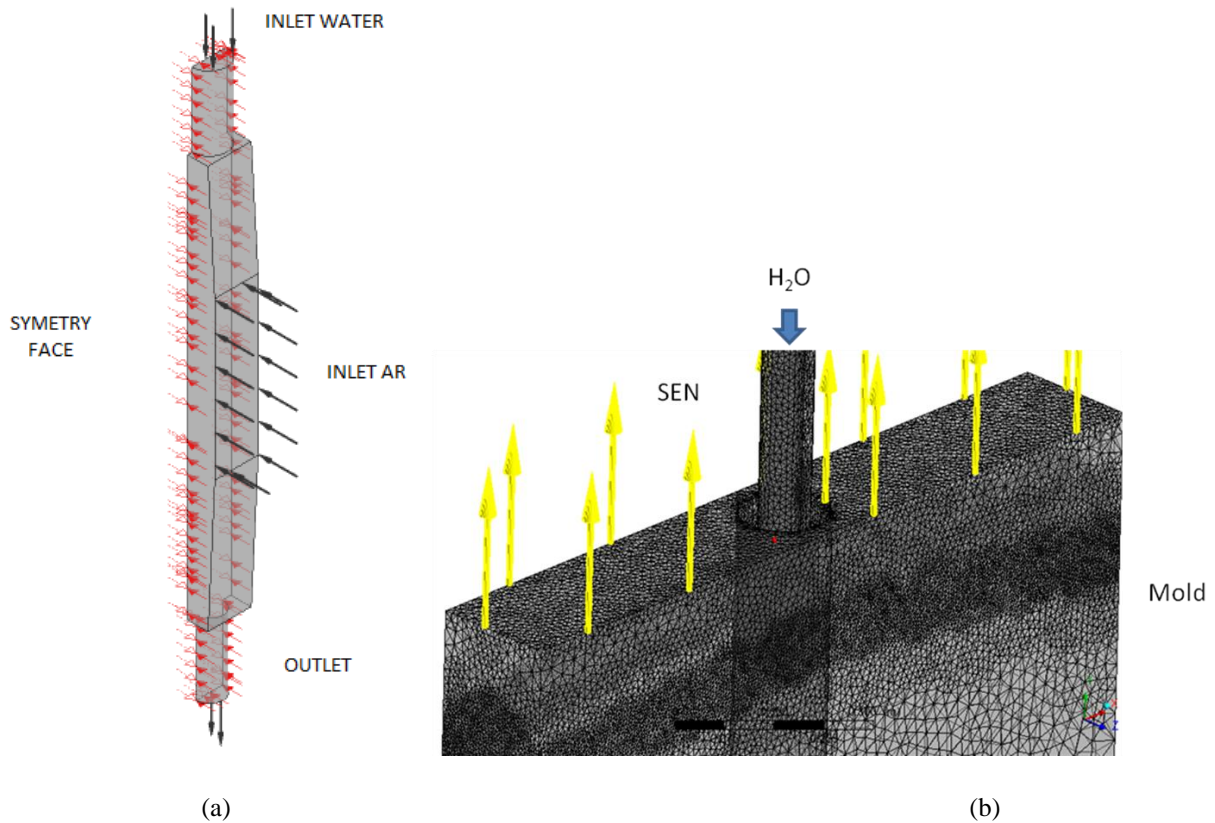(a)   (b)

Figure 2: Image generated by CFX to validate the setup for bubble air / water behavior (a) and mold and submerged nozzle image with emphasis on mesh converted into binary figure.

Finally the configuration of bubble sizes was evaluated with two different ways. As fixed-size bubbles: air was configured as dispersed fluid, with bubbles having a mean diameter of 2.0 mm. For this configuration the bubble diameter remains constant.

Bubble rupture and coalescence using the MUSIG model (Multiple Size Group model considers polydispersed multiphase flows, that means the dispersed phase has a large variation in size and its components interact with each other through the mechanisms of breakup and coalescence; population balance is the established method for calculating the size distribution of a polydispersed phase, including breakup and coalescence effects; see CFX Theory Guide [10]). The MUSIG bubble coalescence and disintegration model is activated when selecting the polydispersed fluid option in the model domain. The bubble medium diameter option is immediately disabled and additional variables representing the minimum and maximum diameter, number of distribution bands and percentage of each range to be adopted must be included in the model. In this work five additional variables representing the bubble diameter bands were added. The minimum diameter of 0.6mm and maximum of 3.2mm were set. These bands were defined based on the mean diameter and deviation obtained through the results of the dynamic physical model for this specific refractory (Santos et al. [5]). The expressions associated with these variables calculate the amount of bubbles in each associated size range and the gas volume fraction in the model.

As discussed by Peixoto et al. [7] and Díaz [12] finding the best combination of drag forces, lift, wall lubrication, turbulent dispersion and virtual mass is fundamental to adequately describe the characteristics of multiphase bubble / liquid flow.

RESULTS AND DISCUSSION

a) Comparison of results of Mathematical Modeling and Physical Model

In the physical model, characterization was done of the behavior of the gas injected through the refractory when being dragged by the water flow. The observation of these conditions, for different air flows and water flows, is fundamental for the adjustment of the mathematical model (Peixoto et al. [11] and Díaz et al. [12]). For a better calibration of the mathematical model, the condition of inverse gravity to the flow of the liquid phase was chosen. As can be seen in Figure 3, increasing the water flow, 40, 60 and 80 l / min, keeps the gas concentration close to the region of the wall and reduces its concentration in the central region. The opposite trend is observed for the increase of the gas flow, from 2 to 5 STPl / min, where the increase of its flow leads to the increase of its penetration in the central regions of the model. Under the experimental conditions here described even with gravity contrary to the liquid flow the gas is always dragged by the liquid phase.
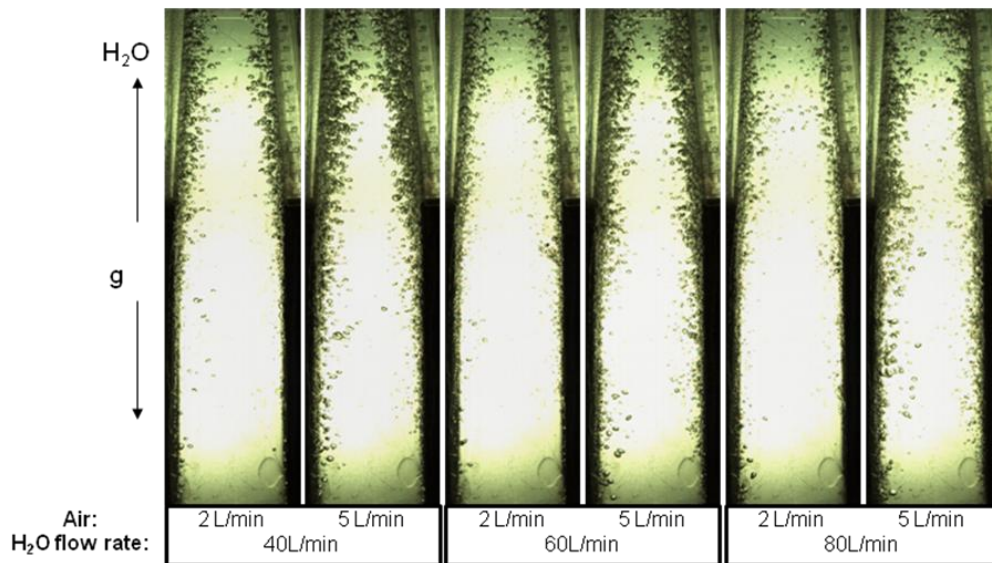

Figure 3. Distribution of gas in the channel with upward liquid flow as a function of gas and liquid flow: g - acceleration of gravity.

Figure 4 shows images of the injection region and model output obtained through mathematical simulation for different combinations of drag and non-drag forces. The drag force was considered in all cases, due to its importance in the viscous flow. For the air flow condition of 5 STPl/min, flow rate of water 80 lpm, and bubble diameter of 2mm, the model was simulated with several adjustments of forces: drag force according model Grace with coefficient equal to -1, Coefficient of Virtual Mass Force (CVMF) equal to 0.5 and 0.25; WLF given by Frank model and TDF model based on the Favre Averaged of the drag force (Ansys 17.1 Setup). The condition with Grace and CVMF equal to 0.5, presented in Figure 4 (a) and (b), did not show displacement of gas flow in the central direction (the flow is concentrated in the vicinity of the wall) as shown in the physical model (Figure 4 - g). For the WLF combined with Grace, VMF, WLF and TDF condition, figure 4 (c), (e) and (f), it is noticed satisfactory results of gas fraction penetration towards the center. When using the Lift Force, figure 4 (d), it is possible to observe two regions of air flow concentration, which is not seen in the physical model (figure 4 h). Among these the condition that best approximates the physical model, removal of the gas from the wall with low concentration in the central region, is represented by Figure 4 (e) with CVMF equal to 0.25 (see shades of light blue after the gas injection region). However, the use of WLF generates a shift of gas concentration (red orange tones) that is not observed in the physical model (higher concentration of gas near the wall). Finally, the best representation was obtained using Grace, CVMF equal to 0.25 and TDF, without using WLF (figure 4 – g).
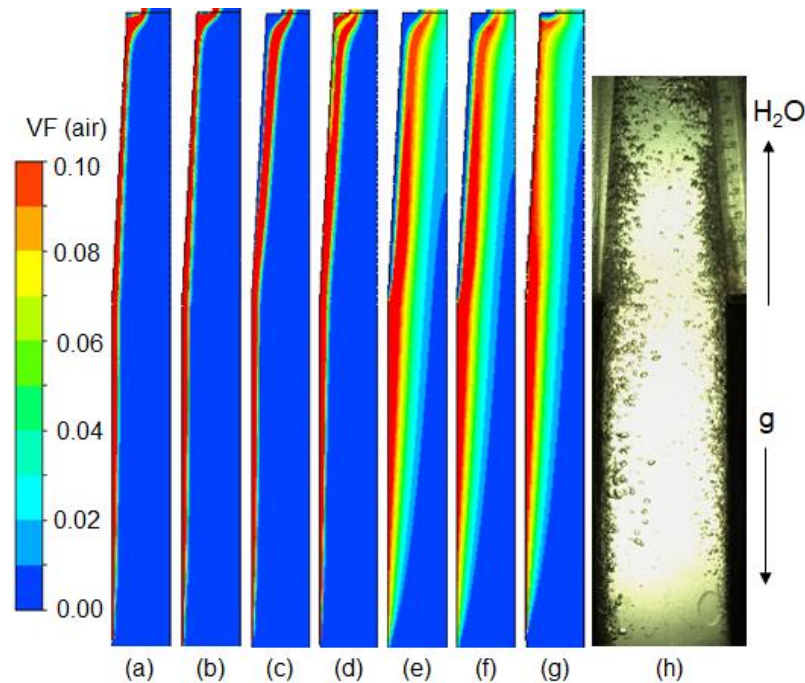
Figure 4:. Distribution of gas in the channel due to the combinations of interphase forces: (a) only drag force given by Grace; (b) Grace + CVMF equal to 0.5; (c) Grace + CVMF equal to 0.5 + WLF given by Frank; (d) Grace + CVMF equal to 0.5 + lift force CL equal 0.5 (e) Grace + CVMF equal to 0.5 + WLF + TDF; (f) Grace + CVMF equal to 0.25 + WLF + TDF; (g) Grace + CVMF equal to 0.25 + TDF; (h) Physical model. Liquid flow rate: 80 L / min; Gas flow rate: 5 L / min. VF is the volumetric fraction.

The mathematical model was also executed with Grace drag force, CVMF equal to 0.25 and TDF, for air flow conditions of 2 and 5 STPl/min and water flow of 40, 60 and 80 lpm. The results are given in Figure 5. Theses resemble to the images obtained for the same conditions in the physical model shown in Figure 3. The increase in gas flow, 2 to 5 STPl / min, (Figure 5 (a) and (b), (c) and (d), (e) and (f)) implies in a increasing concentration of the volumetric fraction in the central region. While the increase in water flow, 40, 60 and 80 lpm, presented a reduction of the volumetric fraction in the central region, both for 2STPl / min and for 5 STPl / min.

Figures 6 (a and b) and 6 (c and d) present the gas distribution images, physical and mathematical model, with gas flow of 1 and 2 STPL / min and water flow of 110 L / min with gravity in the direction of water flow. This condition is similar to the casting conditions considering the input and output diameters of the physical model. The set of drag and non-drag force used for the mathematical model was the optimized condition mentioned above. The mathematical model was adjusted with fixed bubble diameter of 2mm and the resulting images are given in Figure 6 (a and b). As far as for MUSIG simulations taking minimum diameter of 0.6mm and maximum diameter of 3.2mm, images are given in Figure 6 (c and d). The gas distributions of the two models are similar. However, using the MUSIG function allows the model to better represent the volumetric distribution of air, for example, for the 2STPl / min water inlet condition is possible to observe the existence of gas fraction (top of the image), figure 6 d, which is not observed for the same fixed bubble condition.
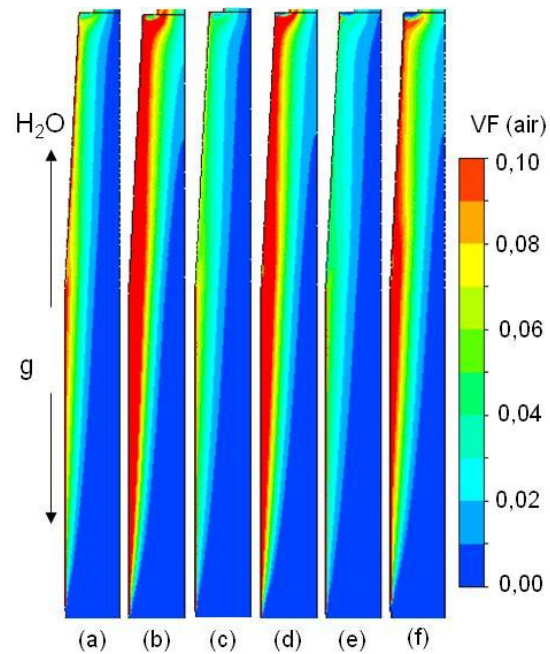
Figure 5. Distribution of gas in the channel as a function of flow: (a) water flow of 40 L / min and air flow of 2 L / min; (b) water flow of 40 L / min and air flow of 5 L / min; (c) water flow of 60 L / min and air flow of 2 L / min; (d) water flow of 60 L / min and air flow 5 L / min; (e) water flow of 80 L / min and air flow of 2 L / min; (f) water flow of 80 L / min and air flow of 5 L / min. Combinations of interphase forces: Grace + CVMF equal to 0.25 + TDF. VF is the volumetric fraction.
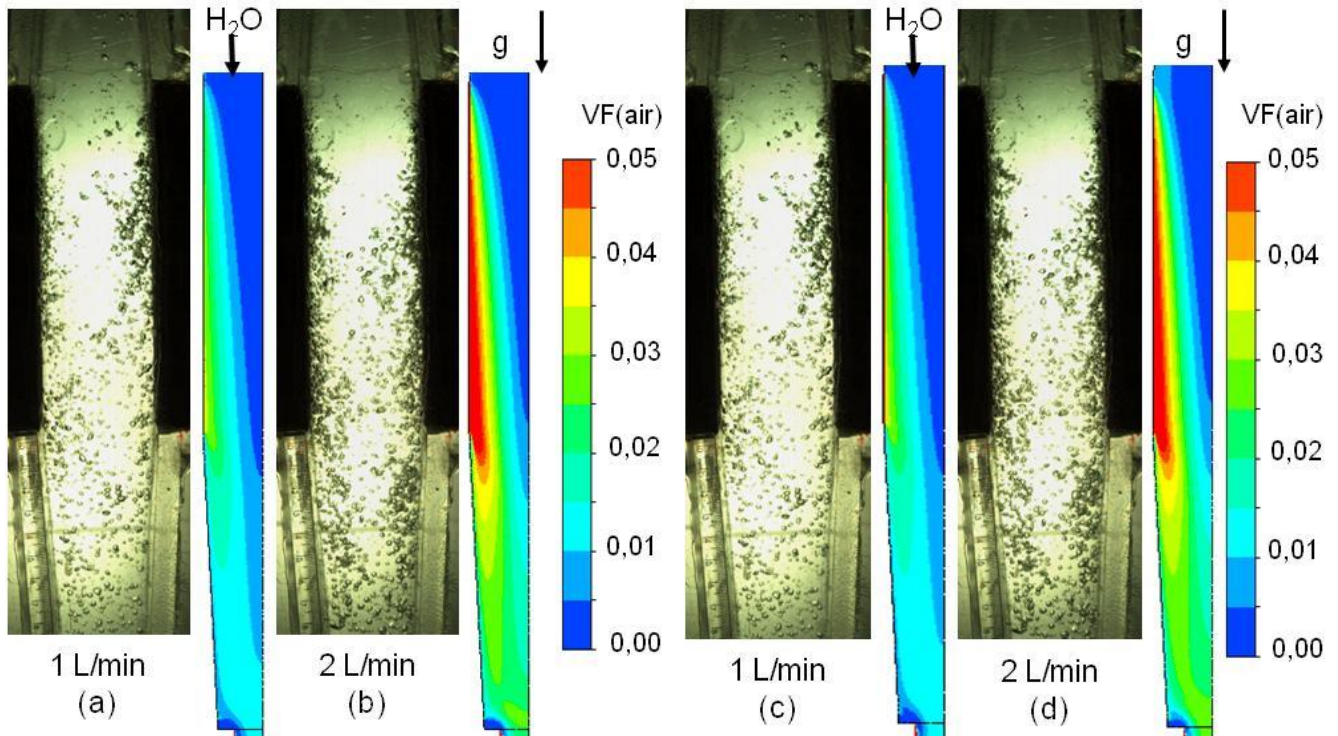
Figure 6: Comparison between physical model and mathematical simulation using fixed diameter (a and b) and MUSIG (c and d) of the gas distribution in the channel with downward flow as a function of the gas flow: (a and c) 1 L / min; (b and d) 2 L / min. Drag force given by Grace + CVMF equal to 0.25 + TDF. Liquid flow rate: 110 L / min. VF is the volumetric fraction; g is the acceleration of gravity.

b) Mathematical Modeling representing the Continuous Casting System

The results of the mathematical model of continuous casting nozzle - mold system are shown in figures 7, 8 and 9 for the conditions of 336 l/min and 400 l/min water flow with injection of 12 l / min of air in the upper nozzle. These parameters represent the usual production conditions for ultra low carbon steel (Santos et al. [9]). In the mathematical model a minimum bubble diameter of 0.6 mm and a maximum of 3.2 mm for MUSIG function have been used. This distribution of bubbles represents the refractory with 928 cD permeability (Santos et al. [5]).

Figure 7 (a) shows the flow vectors and their velocity for condition of 336 l/min of water flow and 12 l/min of air. For this condition the formation of the double roll flow is impaired as the upward movement of the bubbles near the outlet the SEN generates a distortion of the movement of the upper roll. This effect reduces the velocity of the meniscus and reverses its direction in the vicinity of the submerged nozzle (SEN). The same phenomenon is also observed for the condition of 400 l/min with 12 STPl/min but with reduced effect (Figure 7 - b). A modification of the central and upper flow was observed at 400l/min, which in turn allowed the formation of a double roll with smaller velocities in the mold and meniscus than in the 336l/min condition. These behaviors were observed in a physical model and discussed by Santos et al. [9] and Banderas et al. [13].
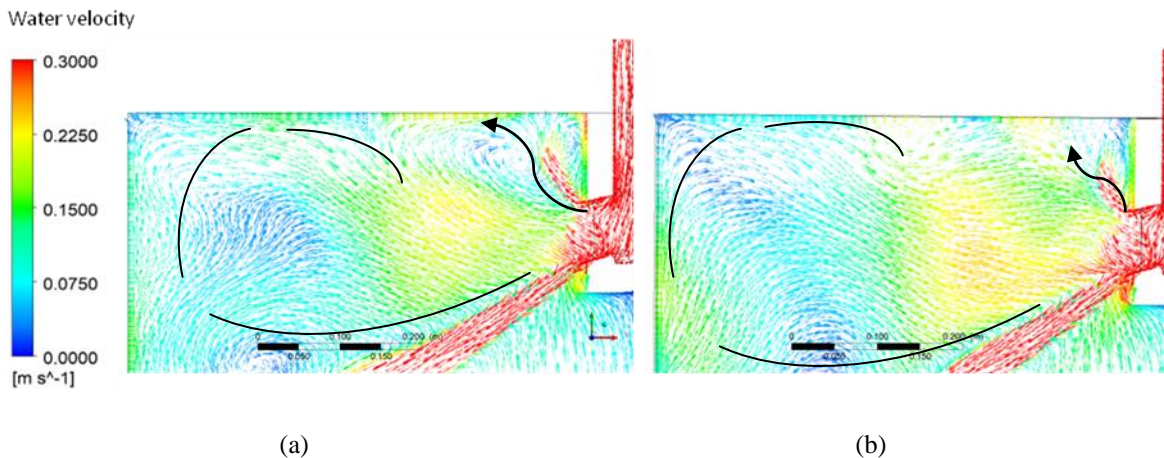

(a)   (b)

 Figure 7: Velocity vectors, 12 STP l / min of air for conditions (a) 336 l / min water and (b) 400 l / min water. Combinations of interphase forces: Grace + CVMF equal to 0.25 + TDF. VF is the volumetric fraction with setup MUSIG.

When comparing the images of Figure 8 of 336 l / min with those of 400 l / min it is seen that the region of the volumetric fraction is much more expanded in the second case. This situation is expected due to the effect of dragging of the gas (dispersed phase) in water (continuous phase) as the water flow increases. However, in addition to the drag effect of water, there is the effect of flow and turbulence on the mean diameter of the bubbles. Figure 9 shows the mean bubble diameter per region at 336 l/min and 400 l/min. For larger water flows, smaller mean bubble diameters are obtained, which allows a more homogeneous dispersion and distribution of the gas phase. This in turn demonstrates that the diameter of the bubble in the mold, and the mechanisms that determine this size, rupture and coalescence of the bubbles, is critical in determining the behavior of the continuous phase and dispersed in the mold. This phenomenon was confirmed in a physical model and also been discussed by Banderas et al. [13], and Santos et al. [9].

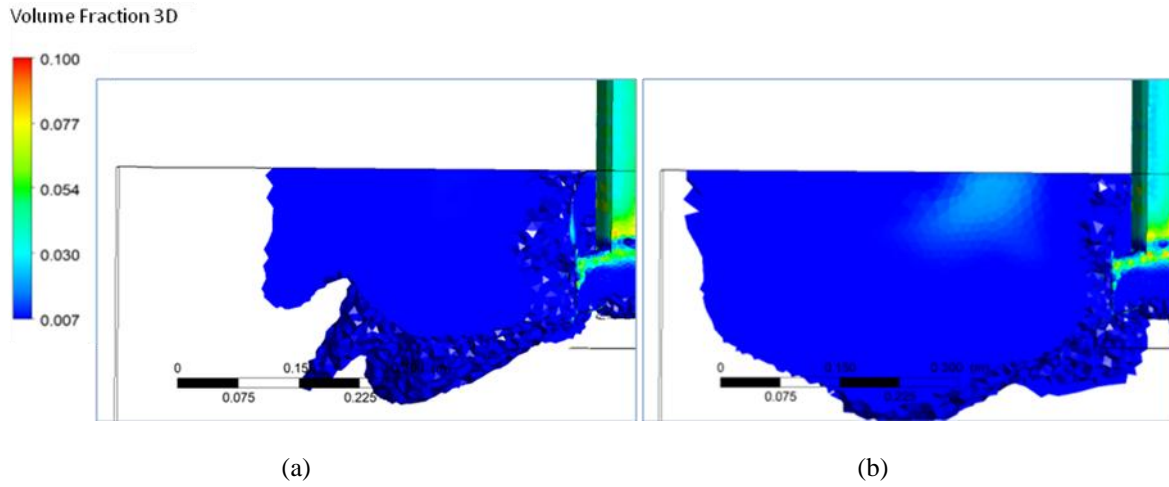(a)   (b)

Figure 8: Volumetric fraction, with 12 STP l/min of air for conditions (a) 336 l/min water and (b) 400 l/min water. Combinations of interphase forces: Grace + CVMF equal to 0.25 + TDF. VF is the volumetric fraction with setup MUSIG.
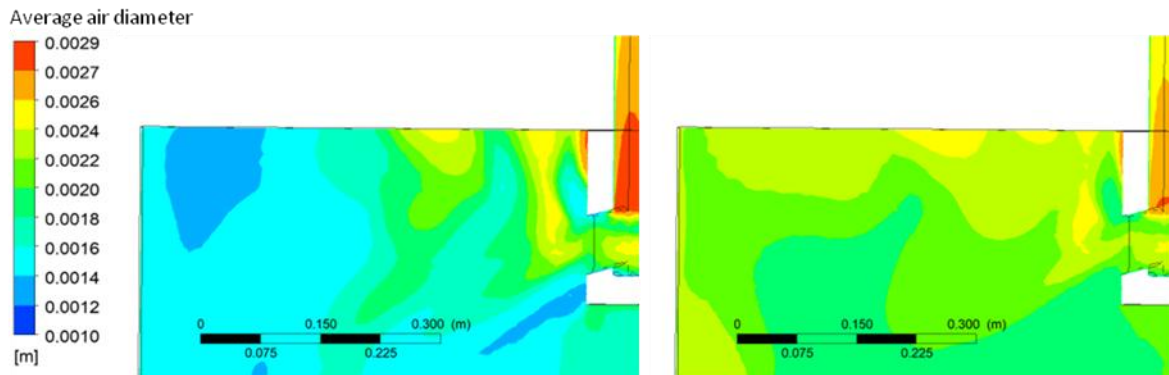

Figure 9: Mean bubble diameter for conditions of 12 STPl/min with (a) 336 l/min water and (b) 400 l/min water. Combinations of interphase forces: Grace + CVMF equal to 0.25 + TDF. VF is the volumetric fraction with setup MUSIG.

Thus the liquid flow rate, for the flow ranges evaluated in this study, influences the process of gas distribution in the mold, besides the direct change of velocity and kinetic energy of the jet at the exit of the nozzle, and also affect the diameter of the bubble in the mold, i.e., higher liquid flows lead to smaller bubble diameters in the mold. This in turn confirms that the mechanism of coalescence and bubble break up at the bottom and the exit of the SEN is a critical factor for determining the average size of the bubble in the mold and plays a fundamental role in defining the flow in the mold. The effect of fluid drag on bubble size is in conformity with findings of SUZUKI et al. [1] and THOMAS et al. [3].

CONCLUSIONS

The best setup for drag forces and no drag for simulation of the bubble / liquid interaction in continuous casting is with Grace coefficient equal to -1, CVMF equal 0.25 and TDF, without using WLF and lift force.

MUSIG model for breakup and coalescence of bubbles refines the solution and allows the mathematical simulation to represent the physical results better.

The mathematical model of continuous casting with the MUSIG function showed continuous (water), dispersed (gas) and medium size bubbles compatible with those observed by Santos et all. [9] and Banderas et all. [13].

ACKNOWLEDGEMENTS

REFERENCES

1. SUZUKI, H; YOSHIMURA, Y; OGATA, M and IMAI, N. *Structure of Porous Upper Nozzle for Tundish and Gas Bublle Behavior*, Shinagawa Technical Report, V 46, p 67- 76, 2003.
2. YUAN, F; WANG, X; ZHANG, J and ZHANG, L. *Numerical simulation of Al2O3 deposition at a nozzle during continuous casting*, Journal of the University of Science and Technology Beijing, Vol 15, Number 3, p. 227, Jun. 2008.
3. THOMAS, B; DENNISOV, A and BAI, H., *Behavior of Argon Bubbles during Continuous Casting of Steel*, ISS 80th Steelmaking Conference, Chicago, 1997, p. 375-384.
4. Lee, G; KIM, S and THOMAS, B. *Investigation of Refractory Properties on the Initial Buble Behavior in the Water Model of Continuous Casting Process.* Materials Science and Technology Conference, AIST/ TMS, Pittsburgh, PA, Oct p 25-29, 2009.
5. SANTOS JUNIOR, P; SILVA, C; DUTRA, P; SANTOS, A; CARVALHO, B; GALINARI, C; SILVA, I. *Influence of the Refractory of the Upper Nozzle in the Behavior of Bubbles in Physical Model of Water – Continuous Casting of Slabs.* 49° Seminário de Aciaria, Fundição e Metalurgia de Não-Ferrosos, Vol 49, São Paulo, Brasil, 2018, p 363 – 374.
6. LIU, R and THOMAS, B. *Model of Gas Flow Through Porous Refractory Applied to an Upper Tundish Nozzle,* The Minerals, Metals & Materials Society and ASM International, volume 46B, February, 2014, p 388 – 405.
7. PEIXOTO, J. et al., *Influência das Forças de Interação Líquido/ Gás na Análise via CFD do Reator RH.* 48º Seminário de Aciaria, Fundição e Metalurgia de Não-Ferrosos, São Paulo, Brasil 2017, p. 356-367.
8. LIU, Z.Q; QI, F.S; LI, B.K; CHEUNGB, S.C.P. *Modeling of Bubble Behaviors and Size Distribution in a Slab Continuous Casting Mold*, International Journal of Multiphase Flow, Vol. 79, China, 2016, p 190-201.
9. SANTOS JUNIOR, P; SILVA, C; SILVA, I. *Distribuição de gás inerte e seu efeito sobre o campo de fluxo durante o lingotamento continuo de placas: modelamento matemático,* Seminário de Aciaria da ABM, Internacional, 2013, Araxá, Brasil.
10. ANSYS. "ANSYS CFX- Theory Guide 17.1", Canonsburg, 2016.
11. PEIXOTO, J.J.M.; GABRIEL, W. V.; OLIVEIRA, T.A.S; SILVA, C.A.; SILVA, I.A.; SESHADRI, V. Numerical Simulation of Recirculating Flow and Physical Model of Slag–Metal Behavior in an RH Reactor: Application to Desulfurization. Metal. and Mat. Transactions B, Vol. 49B, n 5, pp 2421-2434.
12. DÍAZ; M; IRANZO, A; CUADRA, D; BARBERO, R; MONTES, F and GALÁN, M. "Numerical simulation of the gas–liquid flow in a laboratory scale bubble column Influence of bubble size distribution and non-drag forces", *Chemical Engineering Journal*, Vol. 139, 2008, pp. 363–379.
13. BANDERAS, A. R., et al. *Dynamics of two-phase downwards flows in submerged entry nozzle and its influence on the two-phase flow in the mold*, International Journal of Multiphase Flow, Vol. 31, p 643-665, 2005, Mexico.